# Size driven phase transition of barium titanate nanoparticles prepared by plasma chemical vapor deposition

KEIGO SUZUKI, KAZUNORI KIJIMA
*Graduate School of Materials Science and Technology, Kyoto Institute of Technology, Matsugasaki, Sakyo-ku, Kyoto, Japan*

In the displacive-type ferroelectrics such as barium titanate ($BaTiO_3$), it is well known that the crystal structure at room temperature transforms from tetragonal (ferroelectric phase) to cubic (paraelectric phase) with decreasing particle size. This phenomenon is called the "size driven phase transition" in ferroelectrics, and is one of the important phenomena in terms of industry as well as science. Since $BaTiO_3$ nanoparticles have conventionally been prepared by liquid phase methods, numerous researchers have investigated the phase transition behavior using liquid phase synthesized $BaTiO_3$ nanopowder. Various critical sizes of phase transition in the range from 17 to 190 nm have been reported [1–10]. The inconsistency of the critical size is ascribed to the difficulty in measurement, because the difference in lattice constants is less than 0.1 □. Furthermore, factors such as defects, impurities, agglomeration and crystallinity also affect the critical size and total free energies of $BaTiO_3$ nanoparticles. For example, Wada *et al.* reported that the correlational size of dipoles introduced by the hydroxyl groups in the lattice can determine the crystal structure [8, 16, 20]. Buscaglia *et al.* indicated that transition elements doped in $BaTiO_3$ affect the lattice constants [11]. Li *et al.* suggested that agglomeration of $BaTiO_3$ nanoparticles promotes the stability of the tetragonal phase [6]. These are extrinsic factors originating in an imperfection of $BaTiO_3$. Surface energy [10], stress [9] and softening of lattice vibration mode (soft mode) [12] are considered as intrinsic origins of the phase transition.

Recently, we have succeeded in the preparation of $BaTiO_3$ nanoparticles using radio-frequency plasma chemical vapor deposition (RF-plasma CVD) [13]. Well-crystallized $BaTiO_3$ nanoparticles with particle sizes of about 15 nm can be synthesized by this method. The powder has impurities such as strontium of $0.04 \pm 0.01$at%, calcium of $0.08 \pm 0.02$at% iron of $0.05 \pm 0.03$at% and nickel of $0.08 \pm 0.02$at%. Hydroxyl groups were detected on the surface of the particles. The objective of the present work is to clarify the size driven phase transition behavior of the $BaTiO_3$ nanoparticles obtained by the plasma CVD method.

$BaTiO_3$ nanoparticles prepared by the plasma CVD method (as-prepared $BaTiO_3$ nanoparticles) were used as starting materials. The particle sizes were controlled by heating in air at various temperatures of 550, 600, 700, 800, 900 and 1000 °C for 1 hr. The treated powders were identified by X-ray diffraction (XRD) (Model RINT2000 and PSA200, RIGAKU) using $CuK_\alpha$ radiation (1.54051□, 40 kV, 50 mA). The powder morphology was observed using a scanning electron microscope (SEM) (Model S-4000, Hitachi). The degree of grain growth was investigated by specific surface area measurement (SSA) (Model Microtrac surface area analyzer 4200, Nikkisou) with nitrogen absorption. The Ba/Ti atomic ratio was estimated by X-ray fluorescence (XRF) (Model ZSX100E, RIGAKU) using $RhK_\alpha$ radiation (0.61324□, 50 kV, 70 mA). The lattice constants of the treated powders were refined using a Rietveld method. The Rietveld analysis program RIETAN2000 was employed and the fitting of the XRD profile was performed using a pseudo-Voigt function. The crystal structure was also investigated by Raman spectroscopy (Model JRS-system 2000, JEOL) using an Ar laser (514.5 nm, 25 mW).

Fig. 1 shows XRD patterns of the samples treated at various temperatures. An almost single phase of $BaTiO_3$ with a slight amount of barium carbonate ($BaCO_3$) was identified in the samples as-prepared and treated at the temperatures of 550, 600 and 700 °C. On the other hand, single phases of $BaTiO_3$ were obtained by heat treatment at 800, 900 and 1000 °C. Fig. 2 shows SEM images of the samples treated at various temperatures. A remarkable grain growth occurred above 700 °C and the shape of particles in all products was observed to be spherical.

The particle sizes were estimated from SEM images ($d_{SEM}$) and SSA measurements ($d_{SSA}$). Diameters of 100 particles from each of the SEM images were measured and the particle size distribution was fitted using log-normal function. The $D_{50}$ value of particle size distribution was defined as $d_{SEM}$. The results of measured $d_{SEM}$ and $d_{SSA}$ are summarized in Fig. 3. Ba/Ti atomic ratios estimated by XRF measurement are also described in Fig. 3.

Fig. 3 shows that the $d_{SEM}$ and $d_{SSA}$ increased with increasing heat treatment temperature. The $d_{SEM}$ was almost comparable with the $d_{SSA}$ below 800 °C, whereas, the $d_{SSA}$ became much larger than $d_{SEM}$ above 900 °C. This result indicates that particles agglomerate with increasing heat treatment temperature above 900 °C.

The phase transition from cubic to tetragonal causes the peak splitting of the $\{2\ 0\ 0\}_c$ into the $\{2\ 0\ 0\}_t$ and $\{0\ 0\ 2\}_t$ in the XRD profile. Therefore, the phase transition can be confirmed by {2 0 0} peak splitting. To investigate the peak splitting, XRD measurement at a scanning rate of 0.1 °/min in the $2\theta$ range from 44 to 46 ° was carried out. Fig. 4 shows dependence of the

0022–2461  

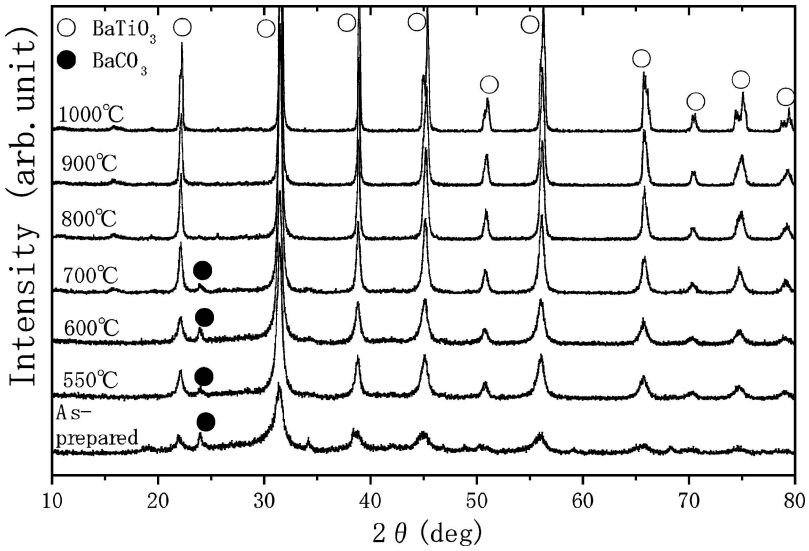


*Figure 1* XRD patterns of the samples treated at various temperatures. $BaTiO_3$ nanoparticles prepared by the plasma CVD method (as-prepared $BaTiO_3$ nanoparticles) were used as starting materials. Heat treatment was carried out in air for 1 hr to control particle size.

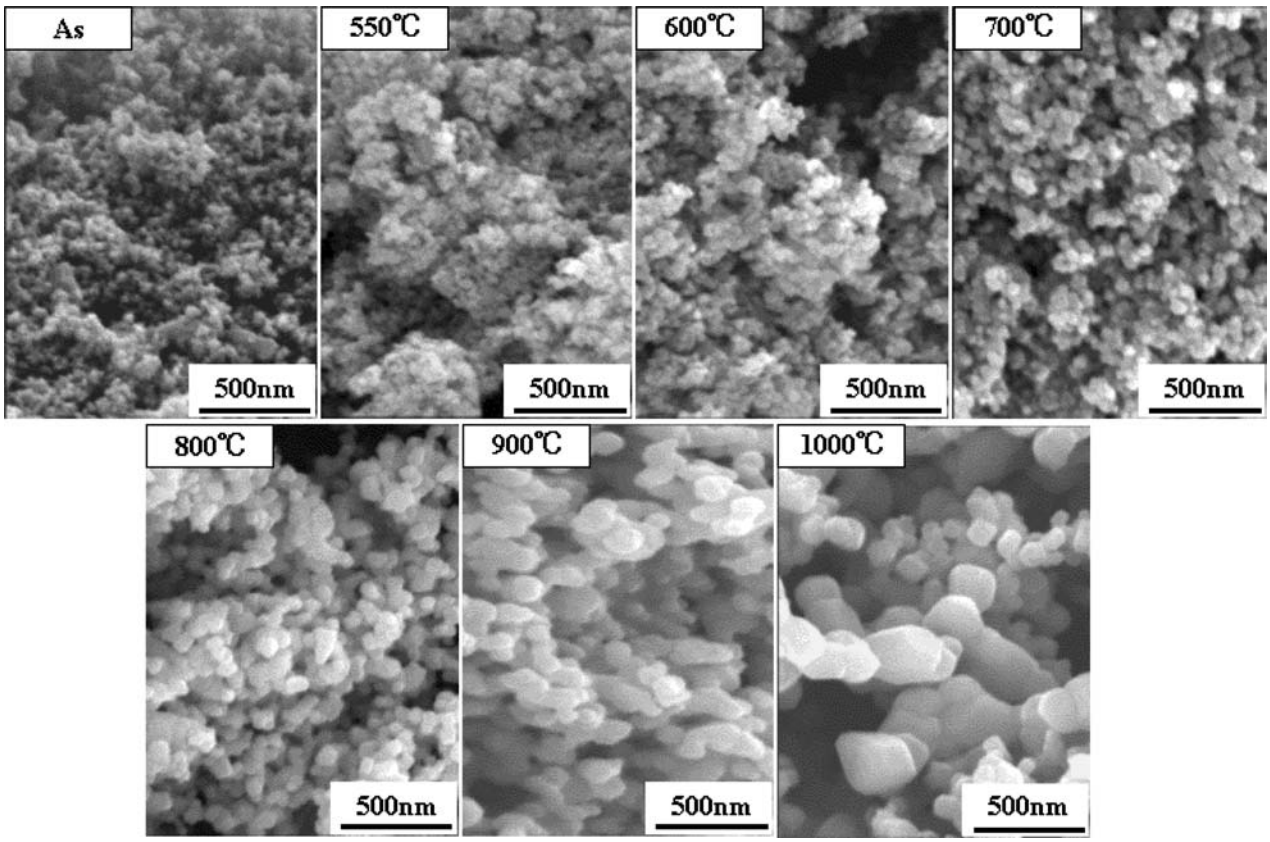


*Figure 2* SEM images of $BaTiO_3$ particles treated at various temperatures.

{2 0 0} peaks of the heat-treated $BaTiO_3$ particles on $d_{SEM}$. In the range of particle size from 21.6 nm (as-prepared) to 68.8 nm (800 °C), only one symmetric peak was observed. However, an asymmetric shape of {2 0 0} peak owing to the peak splitting was confirmed in the sample of 101.2 nm (900 °C). Two peaks ($\{0\,0\,2\}_t$ around 44.9 ° and $\{2\,0\,0\}_t$ around 45.4 °) were observed in the sample of 140.7 nm (1000 °C).

However, it is difficult to determine the crystal structure using only the peak profile of the {2 0 0}. Thus, the crystal structure of the heat-treated samples was refined using a Rietveld method. The analysis was performed for the following two cases: (I) the crystal structure was assumed to be cubic single phase; (II) the crystal structure was assumed to be tetragonal single phase. Table I shows the reliability factors of the analysis. The reliability factors for each result were compared and the crystal structure with higher reliability was adopted as the equilibrium phase at room temperature.

Fig. 5 shows the dependence of lattice constants and tetragonality (lattice constant ratio of *c*-axis to *a*-axis) on $d_{SEM}$. Tetragonality is a commonly used index which describes ferroelectricity. In the sample of 140.7 nm (1000 °C), the lattice constants for the *c*-axis and the

TABLE I Reliability factors of Rietveld analysis for various treated temperatures

| Treated temperature | As prepared | 550 °C | 600 °C | 700 °C | 800 °C | 900 °C | 1000 °C |
|---|---|---|---|---|---|---|---|
| *S* (cubic)* | 2.284 | 2.013 | 1.904 | 1.716 | 1.697 | 1.855 | 3.002 |
| *S* (tetra)* | 2.286 | 1.984 | 1.891 | 1.693 | 1.536 | 1.488 | 1.690 |

*In the present experiment, the reliability factor $S(=R_{wp}/R_e)$ was applied [14]. The lower value of *S* means higher reliability of the analysis. "*S* equals to 1" shows that the refinement of lattice parameters was carried out perfectly.

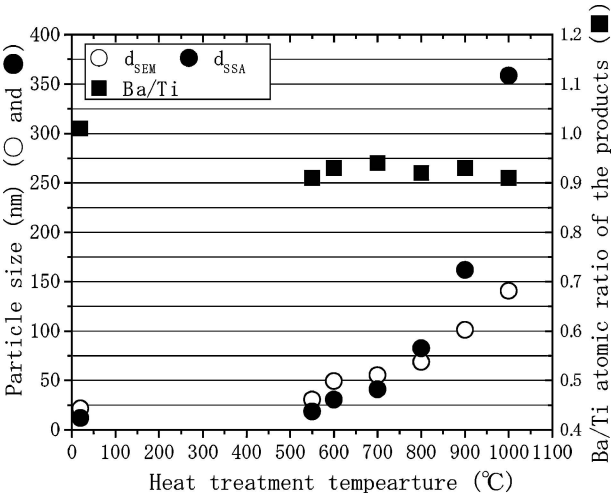


*Figure 3* $d_{SEM}$, $d_{SSA}$ and Ba/Ti atomic ratio of the samples treated at various temperatures. The $d_{SEM}$ and $d_{SSA}$ were the particle size estimated from SEM image and SSA measurement, respectively. Ba/Ti atomic ratio was estimated from XRF measurement.

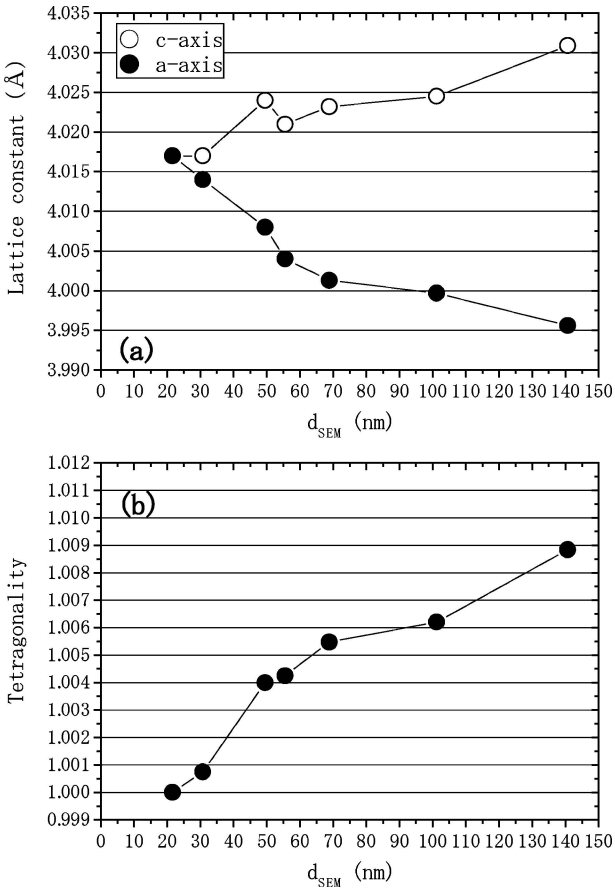


*Figure 5* $d_{SEM}$ dependence of lattice parameters calculated by a Rietveld method: (a) lattice constant (b) tetragonality (the lattice constant ratio of *c*-axis to *a*-axis). The Rietveld analysis program RIETAN2000 was employed and the fitting of the XRD profile was performed using a pseudo-Voigt function.

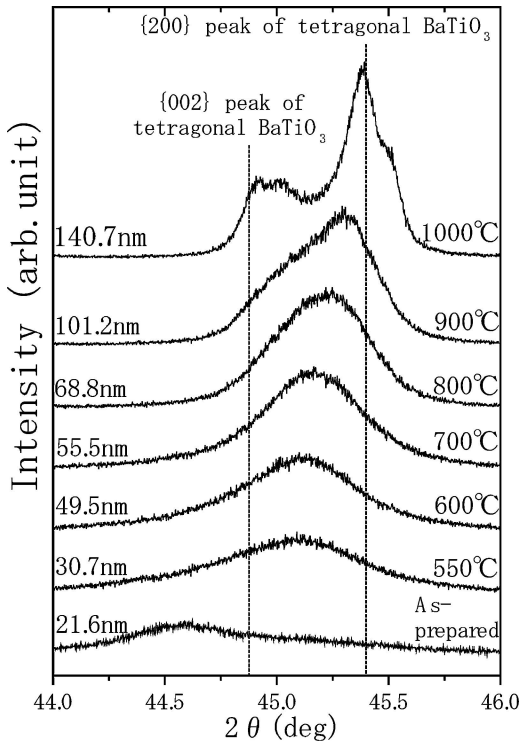


*Figure 4* Dependence of the {2 0 0} peaks of the heat-treated $BaTiO_3$ nanoparticles on $d_{SEM}$. XRD measurement was performed at a scanning rate of 0.1 °/min in the $2\theta$ range from 44 to 46 °. The {0 0 2} and {2 0 0} of the tetragonal phase exist at around 44.9 and 45.4 °, respectively.

*a*-axis were calculated to be 4.031□ and 3.996□, respectively. With decreasing $d_{SEM}$, the lattice constant for the *c*-axis decreased and the lattice constant for the *a*-axis increased. Finally, the *c*-axis lattice parameter corresponded to that for the *a*-axis (= 4.017□) in the sample of 21.6 nm (as-prepared). In the case of bulk $BaTiO_3$, the lattice constant of the cubic phase at room temperature is known to be 4.005□ [15], which was obtained by the extrapolation of the *a*-axis lattice parameter of the cubic phase, stable above Curie point, to room temperature. Therefore, the crystal structure of the as-prepared sample was confirmed to be cubic with an expanded lattice constant compared with bulk cubic $BaTiO_3$. Size driven lattice expansion has also been confirmed in liquid phase synthesized $BaTiO_3$ nanoparticles [16, 17]. This result suggests that lattice expansion is a general phenomenon in the size driven phase transition of $BaTiO_3$.

The tetragonalities in the sample of particle sizes 21.6 nm (as-prepared) and 30.7 nm (550 °C) were estimated to be 1.000 and 1.0007 (±0.0005), respectively. Therefore, the critical particle size of phase transition is considered to be from 21.6 to 30.7 nm (11.9–18.7 nm in $d_{SSA}$). Above the critical size, tetragonality gradually increased with increasing particle size and approached 1.011 (which is the tetragonality of bulk $BaTiO_3$).

Raman spectroscopy is a useful method for studying phase transition. In the tetragonal $BaTiO_3$ (P4mm),

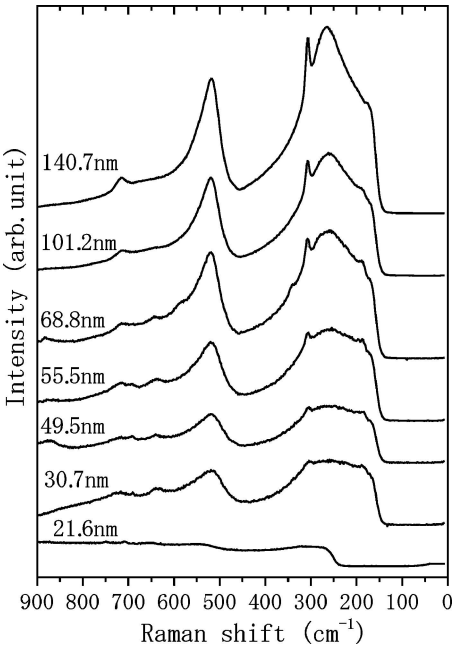


*Figure 6* Dependence of Raman spectra on $d_{SEM}$. The Raman peaks in tetragonal $BaTiO_3$ powder are 720, 515, 305 and 260 $cm^{-1}$. The tetragonal peak of 185 $cm^{-1}$ □ cannot be detected because of apparatus limitations in the present study.

there are Raman active lattice vibration modes, while in cubic (Pm3m) there is no Raman active mode [18]. The Raman peaks in tetragonal $BaTiO_3$ powder are 720 $cm^{-1}$(E(4LO) + $A_1$ (3LO)), 515 $cm^{-1}$ (E(4TO) + $A_1$(3TO)), 305 $cm^{-1}$ (E(3TO) + E(2LO) + $B_1$), 260 $cm^{-1}$ ($A_1$(2TO)) and 185 $cm^{-1}$ (E(2TO) + E(1LO) + $A_1$(1TO) + $A_1$(1LO)) [19], where the lattice vibration modes are shown in parentheses. Using the present Raman spectroscopy apparatus, however, the peak of 185 $cm^{-1}$ cannot be observed, because the Raman scattering light in the range from 0 to 250 $cm^{-1}$ is attenuated owing to a notch filter which cuts off the Rayleigh scattering light.

Fig. 6 shows the Raman spectra for various particle sizes. In the sample of particle size 21.6 nm (as-prepared), the tetragonal peak was not observed at all, i.e., the crystal structure is completely cubic. In the sample of particle size 30.7 nm (550 °C), however, the tetragonal peaks of 720, 515 305 and 260 $cm^{-1}$ were confirmed. Raman spectroscopy can reveal the symmetry of only one unit cell in a crystal [20], therefore, the tetragonal unit cells are supposed to appear around 30 nm. Above 30.7 nm, the peak shapes became sharper with increasing particle size. Therefore, the phase transition is considered to occur in the range from 21.6 to 30.7 nm (11.9–18.7 nm in $d_{SSA}$). This result is in good agreement with the result of the Rietveld method.

The present study clarified the size driven phase transition behavior of $BaTiO_3$ nanoparticles prepared by RF-plasma CVD for the first time.

## References


1. S. W. LU, B. I. LEE, Z. L. WANG and W. D. SAMUELS, *J. Cryst. Growth* **219** (2000) 269.
2. S. WADA, H. CHIKAMORI, T. NOMA, T. SUZUKI and T. TSURUMI, *J. Ceram. Soc. Jpn.* **108** (2000) 728.
3. D. MCCAULEY, R. E. NEWNHAM and C. A. RANDALL, *J. Amer. Ceram. Soc.* **81** (1988) 979.
4. Y. SAKABE, N. WADA and Y. HAMAJI, *J. Korean Phys. Soc.* **32** (1998) S260.
5. Y. FUKUI, S. IZUMISAWA, T. ATAKE, A. HAMANO, T. SHIRASAKI and H. IKAWA, *Ferroelectrics* **203** (1997) 227.
6. X. LI and W. H. SHIH, *J. Amer. Ceram. Soc.* **80** (1997) 2844.
7. H. HSIANG and F. S. YEN, *ibid.* **79** (1996) 1053.
8. S. WADA, T. SUZUKI and T. NOMA, *J. Ceram. Soc. Jpn.* **104** (1996) 383.
9. K. UCHINO, E. SADANAGA and T. HIROSE, *J. Amer. Ceram. Soc.* **72** (1989) 1555.
10. B. D. BEGG, E. R. VANCE and J. NOWOTNY, *ibid.* **77** (1994) 3186.
11. M. T. BUSCAGLIA, V. BUSCAGLIA, M. VIVIANI, P. NANNI and M. HANUSKOVA, *J. Euro. Ceram. Soc.* **20** (2000) 1997.
12. M. R. SRINIVASAN, M. S. MULTANI, P. AYYUB and R. VIJAYARAGHAVAN, *Ferroelectrics* **51** (1983) 137.
13. K. SUZUKI and K. KIJIMA, *Mater. Lett.* to be published.
14. G. S. PAWLEY, *J. Appl. Crystallogr.* **14** (1981) 357.
15. H. F. KAY and P. VOUSDEN, *Philos. Mag.* **40** (1949) 1019.
16. S. WADA, T. SUZUKI and T. NOMA, *Jpn. J. Appl. Phys.* **34** (1995) 5368.
17. S. TSUNEKAWA, S. ITO, T. MORI, K. ISHIKAWA, Z. Q. LI and Y. KAWAZOE, *Phys. Rev. B* **62** (2000) 3065.
18. T. NAKAMURA, T. SAKUDO, Y. ISHIBASHI and Y. TOMINAGA, in "Ferroelectricity Involved in Structural Phase Transitions" (Shokabo, Tokyo, 1988) p. 103.
19. A. SCALABRIN, A. S. CHAVES, D. S. SHIM and S. P. S. PORTO, *Phys. Stat. Soc.* **79** (1977) 731.
20. T. NOMA, S. WADA, M. YANO and T. SUZUKI, *J. Appl. Phys.* **80** (1996) 5223.



*Received 6 February*
*and accepted 19 July 2004*